

# **The Formation of the Solar System by Gravitational Instability: Prediction of a new Planet or Another Kuiper-type Belt**

Evgeny Griv and Michael Gedalin

Department of Physics, Ben-Gurion University of the Negev, P.O. Box 653, Beer-Sheva  
84105, Israel

Received \_\_\_\_\_; accepted \_\_\_\_\_

## ABSTRACT

The early gas–dust solar nebula is considered: the gasdynamic theory is used to study the gravitational Jeans-type instability in its protoplanetary disk. The implications for the origin of the solar system are discussed. It is shown that a collective process, forming the basis of the gravitational instability hypothesis, solves with surprising simplicity the two main problems of the dynamical characteristics of the system, which are associated with its observed spacing and orbital momentum distribution.

*Subject headings:* planetary systems: formation–solar system: formation

## 1. Introduction

Many young stars are surrounded by gas–dust disks (Bodenheimer & Lin 2002). Planetary formation is thought to start with inelastically colliding gaseous and dust particles settling to the central plane of a disk to form a thin and relatively dense layer around the plane. During the early evolution of this disk it is believed that the dust particles coagulate into kilometer-sized rocky asteroids—“planetesimals” ( $\sim 10^{10}$  such bodies) owing to the gravitational instability (Goldreich & Ward 1973) and/or to the collisional sticking (Beckwith et al. 1990). Of these processes, dust particle settling can now be observable.

We suggest that *all* planets of the solar system were created by disk instability. That is, as a result of local gravitational instability, on attaining a certain critical thickness (and density, respectively), small in comparison with the outer radius of the system  $R$ , the circumsolar gas–dust disk disintegrated into a large number of separate protoplanets. Following Boss (2003), this hypothesis envisions coagulation and settling of dust grains within the protoplanets to form rock and ice cores. A protoplanet accreted a gas subsequently from the solar nebula after accumulating a solid core of  $\sim 1 M_{\oplus}$ , followed by the loss of the light elements of the terrestrial planets through the thermal emission of the sun. The advantages of the disk instability model are that (1) the instability process itself is quite fast, and could form planets in  $10^3 - 10^4$  yr (Boss 2002) and (2) in unstable, nonaxisymmetric disks differential rotation can simultaneously transfer angular momentum outward and mass inward through gravitational torques. The work described here has precedents in earlier studies of gravity disturbances in galactic disks and the Saturnian ring disk (e.g., Shu 1970; Lynden-Bell & Kalnajs 1972; Griv, Yuan & Gedalin 1999; Griv, Gedalin & Yuan 2003).

## 2. Dispersion relation

Let us consider the dynamics of the gaseous component in the presence of the collective self-gravitational field. A Langrangian description of the motion of a fluid element under the influence of a spiral field is used, looking for time-dependent waves which propagate in a differentially rotating, two-dimensional disk. The approximation of an infinitesimally thin disk is a valid approximation if one considers perturbations with a radial wavelength that is greater  $h$ , the typical disk thickness (Toomre 1964; Shu 1970; Genkin & Safronov 1975; Safronov 1980).

The time dependent surface density  $\Sigma(\vec{r}, t)$  is split up into a basic and a developing (perturbation) part,  $\Sigma = \Sigma_0(r) + \Sigma_1(\vec{r}, t)$  and  $|\Sigma_1/\Sigma_0| \ll 1$ , where  $r, \varphi, z$  are the cylindrical coordinates and the axis of the disk rotation is taken oriented along the  $z$ -axis. The gravitational potential of the disk  $\mathfrak{N}(\vec{r}, t)$  is also of this form. These quantities  $\Sigma$  and  $\mathfrak{N}$  are then substituted into the equations of motion of a fluid element, the continuity equation, the Poisson equation, and the second order terms of the order of  $\Sigma_1^2, \mathfrak{N}_1^2$  may be neglected with respect to the first order terms. The resultant equations of motion are cyclic in the variables  $t$  and  $\varphi$ , and hence by applying the local WKB method one may seek solutions in the form of normal modes by expanding any perturbation

$$\Sigma_1(\vec{r}, t), \mathfrak{N}_1(\vec{r}, t) = \delta\Sigma, \delta\mathfrak{N} e^{ik_r r + im\varphi - i\omega t} + \text{c. c.}, \quad (1)$$

where  $\delta\Sigma$  and  $\delta\mathfrak{N}$  are the real amplitudes, which are constant in space and time,  $k_r(r)$  is the real radial wavenumber,  $m$  is the nonnegative (integer) azimuthal mode number,  $\omega = \Re\omega + i\Im\omega$  is the complex frequency of excited waves, and c. c. means the complex conjugate. The solution in such a form represents a spiral plane wave with  $m$  arms. The imaginary part of  $\omega$  corresponds to a growth ( $\Im\omega > 0$ ) or decay ( $\Im\omega < 0$ ) of the components in time,  $\Sigma_1$  and  $\mathfrak{N}_1 \propto \exp(\Im\omega t)$ , and the real part to a rotation with constant angular velocity  $\Omega_p = \Re\omega/m$ . Thus, when  $\Im\omega > 0$ , the medium transfers its energy to the growing

wave and oscillation buildup occurs.

It is important to note that in the WKB method, the radial wavenumber is presumed to be of the form

$$k_r(r) = \mathcal{A}\Psi(r), \quad (2)$$

where  $\mathcal{A}$  is a large parameter and  $\Psi(r)$  is a smooth, slowly varying function of the radial distance  $r$ , i.e.,  $d\ln k_r/d\ln r = O(1)$ , and  $|k_r|r \gg 1$ .

Paralleling the analysis leading to equation (34) in Griv et al. (1999), it is straightforward to show that

$$\Sigma_1 = \frac{\beth\Sigma_0}{\omega_*^2 - \kappa^2} \left( k_r^2 + \frac{3\Omega^2 + \omega_*^2 m^2}{\omega_*^2} \frac{m^2}{r^2} + \frac{2\Omega m}{\omega_* r} \frac{\partial \ln \Sigma_0}{\partial r} \right) + \text{c. c.}, \quad (3)$$

where  $\Sigma_1(t \rightarrow -\infty) = 0$ , so by considering only growing perturbations we neglected the effects of the initial conditions,  $\omega_* = \omega - m\Omega$  is the Doppler-shifted (in a rotating reference frame) wavefrequency,  $\Omega(r)$  is the angular velocity of differential rotation at the distance  $r$  from the center, and  $\kappa \approx \Omega$  is the epicyclic frequency. In equation above,  $\beth = \aleph_1 + P_1/\Sigma_0$ ,  $P_1$  is the perturbed gaseous pressure, and  $c = (\partial P/\partial \Sigma)^{1/2}$  is the sound velocity. In equation (3) only the most important low-frequency ( $|\omega_*^2| \lesssim \kappa^2$ ) perturbations developing in the plane  $z = 0$  between the inner and outer Lindblad resonances are considered (Griv et al. 1999, 2003). Equating the perturbed density  $\Sigma_1$  [eq. (3)] to the perturbed density given by the asymptotic ( $k_r^2 \gg m^2/r^2$ ) solution of the Poisson equation (Griv et al. 1999), the Lin–Shu-type dispersion relation is obtained

$$\omega_{*1,2} \approx \pm p|\omega_J| - 2\pi G \Sigma_0 \frac{\Omega}{\omega_J^2} \frac{m}{r|k|L}, \quad (4)$$

where  $p = 1$  for gravity-stable perturbations with  $\omega_*^2 \approx \omega_J^2 > 0$ ,  $p = i$  for gravity-unstable perturbations with  $\omega_J^2 < 0$ ,  $L = (\partial \ln \Sigma_0 / \partial r)^{-1}$  is the radial scale of spatial inhomogeneity,  $|kL| \gg 1$ , and the term involving  $L^{-1}$  is the small correction. Also,

$$\omega_J^2 = \kappa^2 - 2\pi G \Sigma_0 (k_*^2 / |k|) + k_*^2 c^2 \quad (5)$$

is the squared Jeans frequency,  $k = \sqrt{k_r^2 + m^2/r^2}$  is the total wavenumber,  $k_*^2 = k^2 \{1 + [(2\Omega/\kappa)^2 - 1] \sin^2 \psi\}$  is the squared effective wavenumber, and  $\psi = \arctan(m/rk_r)$  is the perturbation pitch angle.

Equation (4) determines the spectrum of oscillations. In the gravity-unstable case, the equilibrium parameters of the disk and the azimuthal mode azimuthal mode number  $m$  ( $=$  number of spiral arms) determine the spiral pattern speed of Jeans-unstable perturbations (in a rotating frame):

$$\Omega_p \equiv \Re \omega_* / m \approx 2\pi G \Sigma_0 \frac{\Omega}{|\omega_J^2|} \frac{1}{r|k|L}, \quad (6)$$

where  $2\pi G \Sigma_0 |k| \sim \Omega^2$ ,  $|\omega_J^2| \sim \Omega^2$ ,  $rk^2|L| \gg 1$ , and, therefore,  $\Omega_p \sim \Omega / rk^2 L \ll \Omega$ . Thus, the typical pattern speeds of spiral structures in Jeans-unstable,  $\omega_J^2 < 0$ , disks are only a small fraction of some average angular velocity  $\Omega_{av}$ . Because  $\Omega_p$  does not depend on  $m$ , each Fourier component of a perturbation in an inhomogeneous system will rotate with the same constant angular velocity. The theory states that in homogeneous ( $|L| \rightarrow \infty$ ) disks  $\Omega_p = 0$ .

The disk is Jeans-unstable to both axisymmetric (radial) and nonaxisymmetric (spiral) perturbations if  $c < c_T$ , where  $c_T = \pi G \Sigma_0 / \kappa$  is the Safronov–Toomre (Safronov 1960, 1980; Toomre 1964) critical velocity dispersion to suppress the instability of axisymmetric ( $\psi = 0$ ) perturbations. Thus, if the disk is thin,  $c \ll r\Omega$ , and dynamically cold,  $c < c_T$ , then such a model will be gravitationally unstable, and it should almost instantaneously (see below for a time estimate) taken on the form of a cartwheel. The instability, which is algebraic in nature, is driven by a strong nonresonant interaction of the gravity fluctuations (e.g., those produced by a spontaneous perturbation and/or a satellite system) with the bulk of the particle population, and the dynamics of Jeans perturbations can be characterized as a nonresonant interaction, that is, in equation (3),  $\omega_* - l\kappa \neq 0$ , where  $l = 0, \pm 1$ .

A very important feature of the instability under consideration is the fact that it is

almost aperiodic ( $|\Re\omega_*/\Im\omega_*| \ll 1$ ). The growth rate of the instability is relatively high:

$$\Im\omega_* \approx \sqrt{2\pi G\Sigma_0(k_*^2/|k|)} \quad (7)$$

and in general  $\Im\omega_* \sim \Omega$ , that is, the instability develops rapidly on a dynamical time scale (on a time of  $3 - 4$  disk rotations, or about  $10^4$  yr in the early solar nebula). From equation (5), the growth rate of the instability has a maximum at the wavelength  $\lambda_{\text{crit}} \approx 2c^2/G\Sigma_0$ . At the boundary of instability, that is,  $c \approx c_T$ ,  $\lambda_{\text{crit}} \approx 2\pi^2 G\Sigma_0/\kappa^2 \sim 2\pi h$ . It means that of all harmonics of initial gravity perturbation, one perturbation with  $\lambda_{\text{crit}} \approx 2\pi h$ , with the associated number of spiral arms  $m$ , and with the pitch angle  $\psi$  will be formed asymptotically in time after a single rotation ( $\approx 5 \times 10^9$  yr ago). For the parameters of the solar nebula ( $R \sim 300$  AU,  $\kappa = 2\pi/T_{\text{orb}} \sim 10^{-10}$  s $^{-1}$ , and the total mass of the disk  $M_d \sim 0.1 M_\odot$ ), one obtains the typical mass of the core of a protoplanet  $M_c \sim 10^{-6} M_\odot \sim M_\oplus$ .

### 3. Spacing of the planets

There exists the empirical Titius-Bode (TB) rule which gives the mean orbital distances of the planets and which can be written in the Blagg–Richardson formulation as

$$r_n = r_0 A^n, \quad (8)$$

where  $r_n$  is the distance of the  $n$ th planet from the Sun (in AU),  $n = 1$  for Mercury, 2 for Venus, ..., and 9 for Neptune,  $A = 1.73$  is the mean ratio between two consecutive planetary distances, and  $r_0 \approx 0.21$ . Also, one cannot overlook the fact that many of the regularities which are found in the planetary system are also to be seen in the regular satellite systems of Jupiter, Saturn, and Uranus, e.g., the spacing of the regular satellites is a variation of the TB rule (Fig. 1). This suggests that the same cosmogonic process must have been responsible for the origin of both types of systems. Lynch (2003) has

already argued that it is not possible to conclude unequivocally that laws of TB type are, or are not, significant. Therefore, the possibility of a physical explanation for the observed distributions remains open.<sup>1</sup>

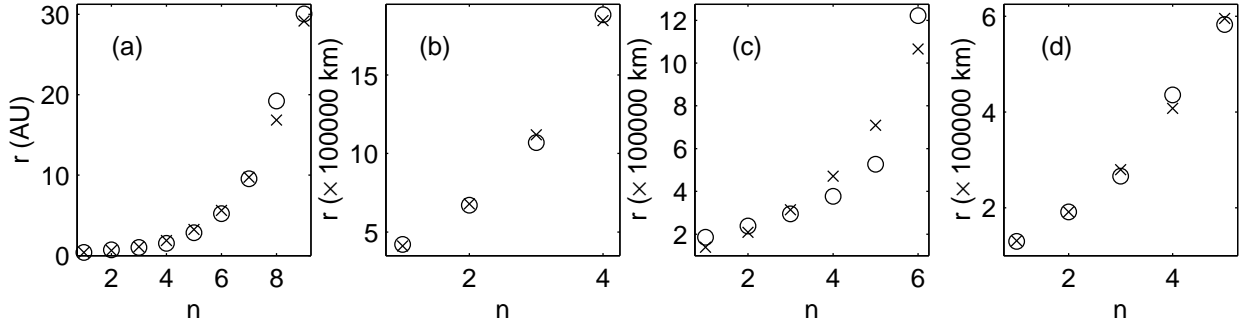


Fig. 1.— Relation between distances of planets (satellites) from the Sun (planets)  $r$  and their numbers  $n$ . Data observed are represented by circles: (a) the solar system, (b) the satellite system of Jupiter,  $r_0 = 249.679$  and  $A = 1.649$ , (c) the satellite system of Saturn,  $r_0 = 92.416$  and  $A = 1.503$ , and (d) the satellite system of Uranus,  $r_0 = 89.737$  and  $A = 1.46$ . The crosses represent the TB rule, equation (8).

Equation (8) can be rewritten:

$$(2\pi / \ln 1.73) \ln(r_n / 0.21) = 2\pi n. \quad (9)$$

Next, the surface density of the disk may be represented in the form of the sum of the equilibrium surface density  $\Sigma_0(r)$  and the perturbed surface density

$$\Sigma_1(r) = \delta\Sigma(r) e^{\Im\omega t} \cos [11.5 \ln(r_n / 0.21) + m\varphi], \quad (10)$$

---

<sup>1</sup>Interestingly, the mean orbital distance to the recently discovered classical Edgeworth–Kuiper belt objects,  $r \approx 46$  AU, is in fair agreement with that given by the TB rule for the solar system's 9th planet,  $r_{10} \approx 50$  AU.

where  $\delta\Sigma(r)$  is the amplitude varying slowly with radius, and  $[11.5 \ln(r_n/0.21) + m\varphi]$  represents the phase varying rapidly with radius,

$$|k_r|r \equiv 11.5 |(d/dr) \ln(r_n/0.21)| r \gg 1.$$

Equation (9) and the condition  $\delta\Sigma(r) > 0$  on the initial phase imply that the maximum values of the perturbed density in equation (10) coincide with the positions of all the planets (Fig. 2a).

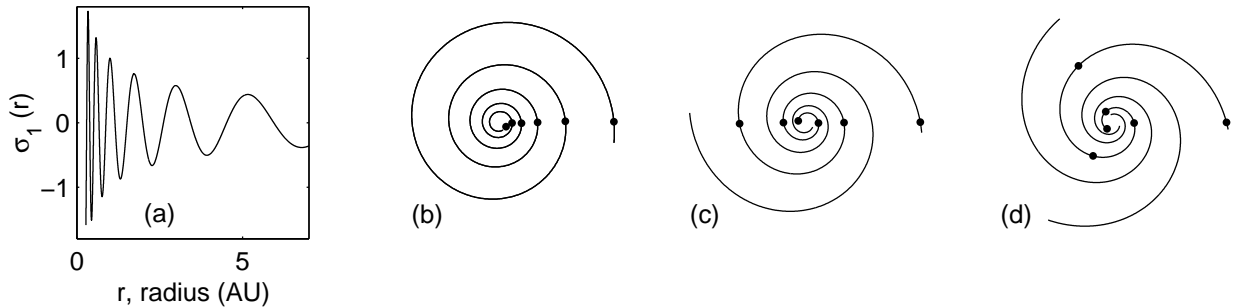


Fig. 2.— (a) Dependence of the perturbed surface density of the protoplanetary disk  $\Sigma_1(r)$  (arbitrary units) on the radius  $r$ , equation (10). The maxima of the perturbed density coincide with locations of all the planets. (b) Spiral density waves with  $m = 1$  arm [eq. (10)] in the  $(r, \varphi)$ -plane, (c) density waves with  $m = 2$  arms, and (d) density waves with  $m = 3$  arms. The filled circles represent the maxima of the perturbed density (protoplanets) of Jeans waves, which are unstable to both axisymmetric and nonaxisymmetric perturbations.

Interestingly, and this is the central part of our theory, the TB rule [eq. (10)] *satisfies* the conditions of the WKB wave with the effective TB radial wavenumber

$$k_{\text{eff}} = \frac{11.5}{r_n}, \quad (11)$$

$d \ln k_{\text{eff}} / d \ln r = O(1)$ , and  $k_{\text{eff}} r \gg 1$  [cf. eq. (2)].<sup>2</sup>

---

<sup>2</sup>Polyachenko (Polyachenko & Fridman 1972) has already been considered this analogy

Thus, if the space dependence of the perturbed surface density of the protoplanetary disk in the  $(r, \varphi)$ -plane has the form of equation (10) with  $\Im\omega > 0$ , the maxima of both radially and azimuthally unstable gravity perturbations are located in places of the solar system's planets (Figs 2b, c, d). Let us define conditions under which the density maxima are localized on planetary orbits. If the disk is inhomogeneous with respect to equilibrium parameters, the wavelength of a perturbation with a maximum growth rate  $\lambda_{\text{crit}}$  will be a function of the radius  $r$ . From the above, the wavelength  $\lambda_{\text{crit}} \approx 4\pi^2 G \Sigma_0 / \kappa^2$ , corresponding to the minimum on the dispersion curve (4) (see also Griv et al. 2003, Fig. 1 therein). On the other hand, the wavelength is  $\lambda_{\text{eff}} = 2\pi/k_{\text{eff}}$ . Comparing  $\lambda_{\text{crit}}$  with  $\lambda_{\text{eff}}$ , we see that in the case where the disk density is dependent on radius according to the law

$$\Sigma_0(r) \approx 0.0138 G^{-1} \kappa^2 r, \quad (12)$$

the maxima of time-increasing, both radially and azimuthally Jeans-unstable density perturbations are arranged in it according the TB rule given by equation (8).

The last condition may be fulfilled in Keplerian disks,  $\kappa \propto r^{-3/2}$ , only if  $\Sigma_0 \propto r^{-2}$ . Interestingly, Tomley et al. (1991) have used almost the same law  $\Sigma_0 \propto r^{-7/4}$  as initial profile for simulation of a disk surrounding the central star. The reason for using such a law comes from a particular model of protostellar cloud collapse Tomley et al. used. It was obtained that this initial model did not get much subsequent evolution in the simulations although it was nicely gravitationally unstable. Based on hydrostatic models, the radial density distributions in circumstellar disks around Herbig Ae/Be and T Tauri stars have been proposed to be in the range  $\Sigma_0 \propto r^{-(1.9-2.4)}$ . Detailed modeling of the

---

in his investigation of the possibility of the explanation of the law of planetary distances by the gravitational instability in sufficiently flat systems, but evidently without success. In particular, Polyachenko studied only axisymmetric  $m = 0$  perturbations, which do not carry angular momentum (see an explanation below in §4).

NIR-to-millimeter appearance of several spatially resolved T Tauri disks has confirmed these predictions. It has been stated that optically thick young disks around those stars with spatial structures are dominated by gravitation and gasdynamics. See, e.g., Stapelfeldt et al. (1998), Chiang & Goldreich (1999), and Wolf, Padgett & Stapelfeldt (2003) for a discussion. Fits of models to observed spectral energy distributions of protostellar disks typically give  $\Sigma_0 \propto r^{-3/2}$  (Bodenheimer & Lin 2002). Also, a standard reference model of a disk, known as the “minimum mass solar nebula,” reconstructed from the distribution of mass in the planets of the solar system and assuming solar composition and no migration of planets, gives  $\Sigma_0 \propto r^{-3/2}$ . The latter is close to the  $r^{-2}$  distribution advocated above. Clearly, given the observational and analytical uncertainties, the two distributions,  $\Sigma_0 \propto r^{-3/2}$  and  $\Sigma_0 \propto r^{-2}$ , are not necessarily inconsistent with each other. For instance, the inclusion of the disk’s self-gravity in addition to the gravitational field of the sun will reduce the value of the exponent  $n$  in the required density–radius relation  $\Sigma_0 \propto r^{-n}$ . In turn, both optical and near-infrared observations of pre-main-sequence stars of intermediate mass have revealed the spiral structure, and thus presumably the Jeans instability, in the circumstellar disks (Grady et al. 1999; Clampin et al. 2003; Fukagawa et al. 2004).

One concludes, therefore, that if the surface density of a protoplanetary disk falls according to the law given by equation (12), the increasing maxima of density perturbations of a Safronov–Toomre-unstable disk ( $c < c_T$ ) are located between the Lindblad resonances in places of the planets (Fig. 2). We believe to have obtained a theoretical interpretation of the TB rule: the distance between planets is the wavelength of the most Jeans-unstable perturbations at the given point of the protoplanetary disk.

By using equation (12), it is easy to find that the disk mass between 0.3 AU and 30 AU is about  $0.4 M_\odot$ . This means that in the present planets there is contained not more than about 0.5% of the mass of the protoplanet cloud. Almost certainly, a part of the initial

mass of the planets was blown away due to intensive corpuscular emission of the early sun.

#### 4. Orbital momentum distribution

We next turn to the question of how to account for the concentration of angular momentum in the planets and of mass in the sun. The torque exerted by the gravity perturbations on the disk is  $\mathcal{T} = - \int \int d^2r (\vec{r} \times \vec{\nabla} \mathfrak{N}_1) \Sigma_1$  or

$$\mathcal{T} = - \int_{r_1}^{r_2} r dr \int_0^{2\pi} \Sigma_1(r, \varphi') \frac{\partial \mathfrak{N}_1(r, \varphi')}{\partial \varphi'} d\varphi'. \quad (13)$$

The points  $r_1$  and  $r_2$  in which  $\omega_* \pm \kappa = 0$  are called the points of inner and outer Lindblad resonances. They play an important role in the theory: the solution of spiral type (1) rapidly oscillating in the radial direction lies between  $r_1$  and  $r_2$ . Outside the resonances,  $r < r_1$  and  $r > r_2$ , the solution decreases exponentially. A special analysis of the solution near corotation ( $\omega_* = 0$ ) and Lindblad resonances is required. Resonances of a higher order,  $\omega_* \pm l\kappa = 0$  and  $|l| = 2, 3, \dots$ , are dynamically of less importance (Shu 1970). To emphasize it again, the present analysis is restricted to consideration of only the principal part of a disk between the Lindblad resonances. Investigation of the wave-particle interaction at spatially limited resonances has been done by Lynden-Bell & Kalnajs (1972), Goldreich & Tremaine (1978, 1980), and Griv, Gedalin, Eichler & Yuan (2000).

Using equation (3), from equation (13) one finds

$$\mathcal{T} \approx - \frac{8\pi \Sigma_0}{\Omega \Im \omega_*} m^2 \mathfrak{N}_1 \mathfrak{N}_1^*, \quad (14)$$

where  $\Im \omega_* > 0$ ,  $\mathfrak{N}_1^*$  is the complex conjugate potential, and the values of  $\mathfrak{N}_1$ ,  $\mathfrak{N}_1^*$ ,  $\Sigma_0$ ,  $\Omega$  are evaluated at  $r = r_1$ . Three physical conclusions can be deduced from equation (14). First, the distribution of the angular momentum of a disk will change under the action of only the nonaxisymmetric forces  $\propto m$ . The latter is obvious: axially symmetrical motions of a

system, studied by Polyachenko, produce no gravitational couples between the inner parts and the outer parts. Second, the distribution of the angular momentum will change upon time only under the action of growing, i.e., Jeans-unstable perturbations ( $\Im\omega_* > 0$ ).<sup>3</sup> Third,  $\mathcal{T} < 0$ : the spiral perturbations remove angular momentum from the disk. This takes place in the main part of the disk between the Lindblad resonances where spiral density waves are self-excited via a nonresonant wave–“fluid” interaction. Further there is absorption of angular momentum by particles that resonate with the wave (Lynden-Bell & Kalnajs 1972). As a result, the bulk of angular momentum is transferred outward (and a mass transported inward, correspondingly). In turn a small group of resonate particles moves outward taking almost all angular momentum.<sup>4</sup> These processes lead to the core-dominated mass density profile in the protoplanetary disk, together with the buildup of an extended, rapidly rotating outer envelope. We speculate that a large portion of the initial mass of the nebula was transported toward the sun.

Let us evaluate the gravitational torque for a realistic model of the protoplanetary disk. In accordance with the theory developed above, the fastest growing spiral mode with  $m \gtrsim 1$ ,  $k_* = k_{\text{crit}}$ , and  $\Im\omega_* \sim \Omega$  is considered. Taking into account that  $8\pi m^2 \aleph_1 \aleph_1^* \sim \aleph_0^2$  (an astrophysicist might well consider a perturbation with  $\aleph_1/\aleph_0$  of 1/10 or even 1/3 to be quite small) and  $\aleph_0 \sim r^2 \Omega^2$ , where  $\aleph_0$  is the basic potential, from equation (14) one obtains  $|\mathcal{T}| \sim \Sigma_0 r^4 \Omega^2$ . The angular momentum of the disk  $\mathcal{L} \sim \Sigma_0 r^4 \Omega$ . Then the characteristic

---

<sup>3</sup>In the opposite limiting case of slow growth ( $\Im\omega_* \rightarrow 0$ ), absorption and emission of angular momentum are confined only to resonate particles (e.g., Lynden-Bell & Kalnajs 1972). The treatment of resonances is beyond the scope of the present analysis.

<sup>4</sup>Lynden-Bell & Kalnajs (1972) have proved that in good conformity with  $N$ -body simulations the gravitational torques can only communicate angular momentum outward if the spirals trails.

time of the angular momentum redistribution is  $t \sim \mathcal{L}/\mathcal{T} \sim \Omega^{-1}$ . Thus, already in the first  $3 - 4$  disk revolutions, in say about  $10^4$  yr, the gas–dust protoplanetary disk sees its almost all angular momentum transferred outward and mass inward. We conclude that the Jeans instability studied here can give rise to torques that can help to clear the nebula on a time scale of  $\gtrsim 1$  Myr, in accord with astronomical requirements. In addition, the analysis is found to imply the existence of a *new* planet (or another Kuiper-type belt) at a mean distance from the sun of  $r_{11} = 0.21 \times 1.73^{11} \approx 87$  AU.

## REFERENCES

Beckwith, S. V. W., Sargent, A. I., Chini, R. S., & Güsten, R. 1990, AJ, 99, 924

Bodenheimer, P., & Lin, D. N. C. 2002, ARE&PS, 30, 113

Boss, A. P. 2002, ApJ, 576, 462

Boss, A. P. 2003, ApJ, 599, 577

Chiang, E. I., & Goldreich, P. 1999, ApJ, 519, 279

Clampin, M., Krist, J. E., Ardila, D. R., et al. 2003, AJ, 126, 385

Fukagawa, M., Hayashi, M., Tamura, M., et al. 2004, ApJ, in press

Genkin, I. L., & Safronov, V. S. 1975, Soviet Ast., 19, 189

Goldreich, P., & Tremaine, S. 1978, Icarus, 34, 240

Goldreich, P., & Tremaine, S. 1980, ApJ, 241, 435

Goldreich, P., & Ward, W. 1973, ApJ, 183, 1051

Grady, C. A., Wootgate, B., Bruhweiler, F. C., Boggess, A., Clampin, M., & Kalas, P. 1999, ApJ, 523, L151

Griv, E., Gedalin, M., Eichler, D., & Yuan, C. 2000, Phys. Rev. Lett., 84, 4280

Griv, E., Gedalin, M., & Yuan, C. 2003, MNRAS, 342, 1102

Griv, E., Yuan, C., & Gedalin, M. 1999, MNRAS, 307, 1

Lynch, P. 2003, MNRAS, 341, 1174

Lynden-Bell, D., & Kalnajs, A. J. 1972, MNRAS, 157, 1

Polyachenko, V. L., & Fridman, A. M. 1972, Soviet Ast., 16, 123

Safronov, V. S. 1960. Ann. d'Astr., 23, 979

Safronov, V. S. 1980, in Early Solar System Processes, ed. D. Lal (Amsterdam: North-Holland), 73

Shu, F. H. 1970, *ApJ*, 160, 99

Stapelfeldt, K. R., Burrows, C. J., Krist, J. E., et al. 1998, *ApJ*, 508, 736

Tomley, L., Casse, P., & Steiman-Cameron, T. 1991, *ApJ*, 382, 530

Toomre, A. 1964, *ApJ*, 139, 1217

Wolf, S., Padgett, D. L., & Stapelfeldt, K. R. 2003, *ApJ*, 588, 373